AUTHOR(S):

TITLE:

YEAR:

Publisher citation:

OpenAIR citation:

Subcutaneous fat patterning in athletes: selection of appropriate sites and standardisation of a novel ultrasound measurement technique: ad hoc working group on body composition, health and performance, under the auspices of the IOC Medical Commission

Wolfram Müller,[1] Timothy G Lohman,[2] Arthur D Stewart,[3] Ronald J Maughan,[4] Nanna L Meyer,[5] Luis B Sardinha,[6] Nuwanee Kirihennedige,[5] Alba Reguant-Closa,[5] Vanessa Risoul-Salas,[5] Jorunn Sundgot-Borgen,[7] Helmut Ahammer,[1] Friedrich Anderhuber,[8] Alfred Fürhapter-Rieger,[1] Philipp Kainz,[1] Wilfried Materna,[9] Ulrike Pilsl,[8] Wolfram Pirstinger,[1] Timothy R Ackland[10]

ABSTRACT

Background Precise and accurate field methods for body composition analyses in athletes are needed urgently.

Aim Standardisation of a novel ultrasound (US) technique for accurate and reliable measurement of subcutaneous adipose tissue (SAT).

Methods Three observers captured US images of uncompressed SAT in 12 athletes and applied a semiautomatic evaluation algorithm for multiple SAT measurements.

Results Eight new sites are recommended: upper abdomen, lower abdomen, erector spinae, distal triceps, brachioradialis, lateral thigh, front thigh, medial calf. Obtainable accuracy was 0.2 mm (18 MHz probe; speed of sound: 1450 m/s). Reliability of SAT thickness sums (N=36): R^2=0.998, SEE=0.55 mm, ICC (95% CI) 0.998 (0.994 to 0.999); observer differences from their mean: 95% of the SAT thickness sums were within ±1 mm (sums of SAT thicknesses ranged from 10 to 50 mm). Embedded fibrous tissues were also measured.

Conclusions A minimum of eight sites is suggested to accommodate inter-individual differences in SAT patterning. All sites overlie muscle with a clearly visible fascia, which eases the acquisition of clear images and the marking of these sites takes only a few minutes. This US method reaches the fundamental accuracy and precision limits for SAT measurements given by tissue plasticity and furrowed borders, provided the measurers are trained appropriately.

BACKGROUND

Body composition has a large impact on health and performance. In aesthetic sports, weight category sports and gravitational sports (in which body weight influences performance, eg, ski jumping, long distance running, etc), many athletes reduce weight rapidly or maintain an extremely low body weight or fat mass in order to gain a competitive advantage. Weight, fatness, energy intake and energy expenditure are closely related to each other. Therefore, extreme weight changes, very low body weight, extremely low body fat content, loss of tissue or insufficient bone mineral density are common in many weight sensitive sports.[1–5] This may induce severe medical problems,[1] [5–7] and instead of the assumed competitive advantage, severe and long-lasting performance setbacks may result.[8–11] The health of the athlete is a precondition for optimum performance. Protecting the health of athletes and optimising their performance both depend on the availability of accurate, precise and valid methods for the assessment of body composition.[12 13]

Recently, the IOC working group on Body Composition, Health and Performance presented a discussion paper on how to minimise risks for athletes in weight sensitive sports.[5] Currently, there are no generally accepted lower limits of weight or fat mass for male and female athletes that can be used as scientifically based threshold values for optimal performance, or for raising the alarm, or for removal of athletes from competition. There are two reasons for this unsatisfactory situation: first, valid methods with sufficient accuracy for body composition assessment in athletes that are applicable in the field do not exist and second, interpretation of body composition data of athletes in various sports is a complex task, particularly because individual differences as well as general sexual dimorphism underpins differences that require consideration.

Body composition data must be seen in the context of other health parameters.[5] Longitudinal changes in body mass (m) and body composition should be followed accurately and precisely for the assessment of the health risks associated with precompetition manipulation of body mass.[5] Subcutaneous adipose tissue (SAT) measurement using skinfolds has a long tradition, but the accuracy obtainable with this technique is limited because skin and SAT are measured together in a compressed state without considering the compressibility and viscous-elastic behaviour at the individual measurement sites.[12–14]

Recently, a novel ultrasound (US) technique for measurement of SAT and embedded fibrous structures has been introduced.[12–15] This US technique avoids

the tissue compression and movement that occurs when using skin-fold callipers and employs a recently developed image evaluation procedure for multiple thickness measurements of SAT layers.

AIMS AND CONTENTS

This US technique and the obtainable accuracy of tissue thickness measurements is analysed in part A. The introduction of a standard set of sites that fulfil the criteria for accurate and reliable measurements of SAT thickness is the content of part B, and interobserver reliability results obtained with this new set of sites in a group of competitive athletes are described in part C. Additional important information on the standardised application of this method for measuring uncompressed SAT thickness and on the interobserver results can be found in the online supplementary appendix.

PART A: US TECHNIQUE AND ACCURACY
B-mode US imaging

B-mode (brightness mode) US images are generated by sequences of US beams which penetrate the tissue to create an image in which the brightness of the screen corresponds to the echo intensity in the plane of the scan. The principle of US imaging is the pulse-echo technique. A short pulse (several wavelengths long) is applied and travels with the speed of sound (c) in a given tissue. Diagnostic US systems conventionally use c=1540 m/s for calculating the distance (d_{US}) from the surface of the probe to the boundary between two tissues. The speed of sound in adipose tissue is lower than that in other soft tissues (1450 m/s).[16 17]

Standardised US imaging of SAT

US was applied to measure subcutaneous fat as early as 1965,[18] and many applications followed[19–24] in which the potential of this method was identified. A brief review of the history of US applied to measure body fat can be found in Müller et al.[14] A novel approach for avoiding measurement errors due to high compressibility of fat[14 25] and a semiautomatic image evaluation procedure designed to minimise measurement errors have recently been published.[12 14 15] Since SAT is highly compressible, the US probe (transducer) has to be placed over a given site without any pressure. This is obtained by using a thick layer of US gel between the probe and the skin (a 3–5 mm thick gel layer should be seen above the skin in the US image). According to the standardised approach applied here, US measurements are made with the participant lying in a supine, prone or rotated position. A diagnostic US system (GE Logic e) with a linear probe operated at 18 MHz (in the harmonic mode) was used for the SAT images in this publication (axial resolution: about 0.10–0.15 mm). The application of the US measuring technique at the individual sites is described in part B (table 1). Important points for avoiding errors when using this standardised US method to measure SAT can be found in online supplementary appendix, part A.

Accuracy of US thickness measurements

Diffraction and technically obtainable minimum pulse length limit lateral and axial resolution approximately to the wavelength used. Diagnostic US probes (transducers) use frequencies from 3 to 22 MHz, which corresponds to a wavelength in soft tissue of 0.5–0.07 mm. US attenuation increases with increasing frequency—typical investigable depths are between 10 mm (22 MHz) and 200 mm (3 MHz). For studies of fat patterning in athletes or other individuals who have only thin layers of SAT, high frequencies (9–18 MHz) are recommended to obtain US images with high resolution. This enables thickness

measurements with an accuracy that is limited only by furrowed borders and plasticity of the tissues. When using 18 MHz, the border resolution error due to the US resolution limit is about 0.1 mm on each side of the SAT. The calculated distance is the sound speed multiplied by half the echo time. Therefore, any deviation of the sound speed used by the US system from the actual sound speed in the tissue adds to the distance measurement error. In obese persons, where SAT is several centimetres thick, the border resolution error can be neglected; accuracy would be limited by incorrect sound speed rather than by US resolution. For instance, when measuring a 100 mm thick SAT layer, it does not matter whether the borders are detected with a resolution of 0.1 or 0.3 mm (corresponding to 0.1%, or 0.3%, respectively). Therefore, a lower frequency (which is necessary for thick tissue layers) will not reduce accuracy substantially, provided the speed of sound is set correctly.

In the distance evaluation algorithm (FAT Software; rotosport.com) developed for multiple tissue thickness measurements, the sound speed can be set appropriately for any biological tissue. Thus, the technical measurement error can be kept very low; this also holds true in thick fat layers. The limiting factors for accuracy are intrinsic in the tissue: furrowed tissue borders and viscous-elastic features of SAT. Since accuracy is limited primarily by these biological factors, and since precision limitations (reliability), not technical US accuracy limitations, will be the dominating factor of the overall error in most cases, it is of paramount importance to minimise these influences by standardising measurement sites and technique (see part B). An example analysis of technically obtainable measurement accuracy can be found in online supplementary appendix, part A. Interobserver reliability is analysed quantitatively for a sample of athletes in part C of this publication.

Semiautomatic multiple thickness measurement of SAT

For measurement of a series of thickness values in a given US image, an image segmentation algorithm for detecting the SAT contour was applied[14] and US images were evaluated by means of a semiautomatic distance measurement algorithm (FAT Software, rotosport.com). Sound speed was set to 1450 m/s in the evaluation software for distance calculation in adipose tissue.[16 17] Usually 50 to 300 individual thickness measurements resulted from one image (depending on the selected region of interest). Mean, SD, median, minimum and maximum values were automatically calculated. The tissue segmentation was controlled visually and, if necessary, parameters that determine the accepted segment inhomogeneity could be set manually to optimise SAT contour detection. The software also enables an operator to distinguish between distances in which embedded tissues (eg, fibrous structures) are included (d_{INCL}) or excluded (d_{EXCL}). The thickness of the embedded structures is also determined: $d_{ES}=d_{INCL}-d_{EXCL}$.

PART B: STANDARDISATION OF US SITES AND PROCEDURE

A new set of sites that provide anatomical and image clarity is presented in this part. An accurate description of these sites and the development of a basis for standardising this US measurement technique are the core of this section.

The US approach to measure SAT outlined in part A was first applied to the set of sites used for skinfold measurement (International Society for the Advancement of Kinanthropometry—ISAK sites), but several of these skinfold sites do not allow clear US images,[14 15] and the marking of ISAK sites requires specific knowledge of anatomy and detailed anthropometry training.[26 27] ISAK sites were defined for skinfold studies, but do not optimally fulfil the criteria for US

Table 1 Description of ultrasound (US) sites and measurement procedure (see figure 1)

Site name	Description of the sites Marking is done in a standing or sitting position, on the right side of the body; see figure 1. All distances (d) are percentages of body height h	Notes on US image capture All US measurements in a lying position! Always use a thick layer of US gel (at least 3–5 mm)
UA Upper abdomen	1. Mark a vertical line at a distance d=0.02 h (ie, 2% of body height h) lateral to the centre of the umbilicus (*omphalion*) 2. Project vertically and mark a horizontal line at d=0.02 h **superior** to the *omphalion* (figure 1A). (In case this site is above a tendinous inscription of the rectus abdominis (where subcutaneous adipose tissue (SAT) is thicker), move the probe some mm to the end of this inscription and measure the thickness there)	Lying in a supine position Have the participant stop breathing at mid-tidal expiration and then capture the image
LA Lower abdomen	1. The same line (1) as for the upper abdomen 2. Project vertically and mark a horizontal line at d=0.02 h **inferior** to the *omphalion*. Measure always exactly at this point (figure 1A)	Lying in a supine position Have the participant stop breathing at mid-tidal expiration and then capture the image
EO External oblique (optional site)	1. Locate and mark the anterior superior iliac spine (ASIS). 2. The participant assists by holding the end of the tape at the apex of the costal arch at the inferior margin of the sternum (where it meets the xiphoid process). The participant looks ahead! 3. Draw a line from the ASIS in the direction of the costal arch 4. Mark a perpendicular line at d=0.02 h from ASIS (figure 1A)	Lying in a supine position Capture the image with the probe held in the direction of the **perpendicular** line
ES Erector spinae	1. Mark a transverse line at d=0.14 h above the solid surface (table) on which the person is sitting in a stretched upper body position with thighs horizontal and legs unsupported 2. Mark the site at d=0.02 h lateral to the spinous process of the vertebra (figure 1C)	Lying in a prone position
DT Distal triceps	1. Put the lower arm on a support surface (table) with the hand in the mid-prone position; mark a vertical line on the most posterior aspect of the arm. 2. Mark the site on the vertical line at a distance from the surface of d=0.05 h (figure 1D)	Lying in a prone position Capture the image with the dorsal surface of the hand on the table. Make sure the probe orientation is perpendicular to the skin
BR Brachioradialis	1. The participant puts the forearm with the hand in the mid-prone ('shake-hands') position on a support table and contracts the brachioradialis (eg, against a resistance provided by the hand of the measurer), figure 1D. 2. Draw a longitudinal line on the most anterior surface of the brachioradialis muscle 3. Mark a transverse line at a distance d=0.02 h distally from the anterior surface of the biceps brachii tendon (press the end of the metre rod onto the stretched tendon). Project this line transversely to intersect with the longitudinal line (figure 1D)	Lying in a supine position Take the image with the arm in a mid-prone position and in contact with the thigh (muscles of the arm are relaxed) Avoid imaging the vein in case there is one in the vicinity
FT Front thigh	1. Put the foot on the anthropometric box which is placed in front of a wall such that the thigh is horizontal and the big toe and the knee touch the wall 2. Mark the site at a horizontal distance d=0.14 h from the wall (figure 1E)	Lying in a supine position.
MC Medial calf	1. Place the foot on the anthropometric box such that the thigh is horizontal and the leg vertical 2. Mark the site at d=0.18 h above the surface at the most medial aspect (use a ruler to determine the most medial aspect when looking vertically down (figure 1F)	Lying in a rotated position Participant rolls onto the right side with the right knee at a 90° angle so that the lateral aspect of the right leg is supported
LT Lateral thigh	1. Draw a horizontal line on the lateral side of the thigh at the height of the gluteal fold (at the height of the fold at the most dorsal aspect of the thigh); 2. Mark the site on this line at the midpoint of the sagittal thigh diameter (figure 1G). Use a calliper for (1) and (2)	Lying in a rotated position Participant rolls onto the left side with both knees at a 90° angle, with the right leg over the left leg

measurement of uncompressed SAT. Therefore, identification of sites that can be found easily and reproducibly, also by those who lack specific anthropometry experience, was necessary for SAT patterning studies using diagnostic US. The search for new sites was determined by the following criteria: the set of sites represents trunk, arms and legs; sites can easily be marked with high precision after 1 h of training; all distances necessary to define the new sites are relative to the person's body height; anatomical structures are easily identifiable in the US image (dermis, SAT, fascia of the muscle); and SAT thickness does not change much in the vicinity of the site.

Description of standard sites selected for US measurements of SAT patterning

Table 1 describes the basic set of eight sites that were selected for analysis of SAT patterning. All sites are marked on the right side of the body (figure 1A–G). The table also includes notes on how to take the US images at the individual sites. Sites UA (upper abdomen), LA (lower abdomen) and EO (external oblique) are marked in the standing position (figure 1A). In the fat patterning studies described in this publication, the EO site

was used. This site is close to the supraspinale ISAK site, but recent experience has shown that SAT layers are very thin at this site in athletes and do not contribute substantially to the sum of SAT thicknesses, and marking takes too much time and can be difficult in obese persons. Therefore, EO should only be used as an optional site in future studies. The site ES (erector spinae) is marked in the stretched sitting position (figure 1C), while sites DT (distal triceps) and BR (brachioradialis) are marked with the forearm supported on a table and the arm held vertically (figure 1D). The site FT (front thigh) is marked with the foot placed on an anthropometric box which is placed in front of a wall such that the thigh is horizontal and the big toe and the knee touch the wall (figure 1E). Site MC (medial calf) is marked with the right foot on a box of appropriate height such that the upper leg axis is horizontal and the lower leg vertical (figure 1F). LT (lateral thigh) should be used in the core set of eight sites to determine SAT thickness in this fat depot area of the thigh. The site is marked in the standing position at the midpoint of the sagittal thigh diameter at the height of the gluteal fold (the height at the most dorsal aspect is used in case the fold is not horizontal).
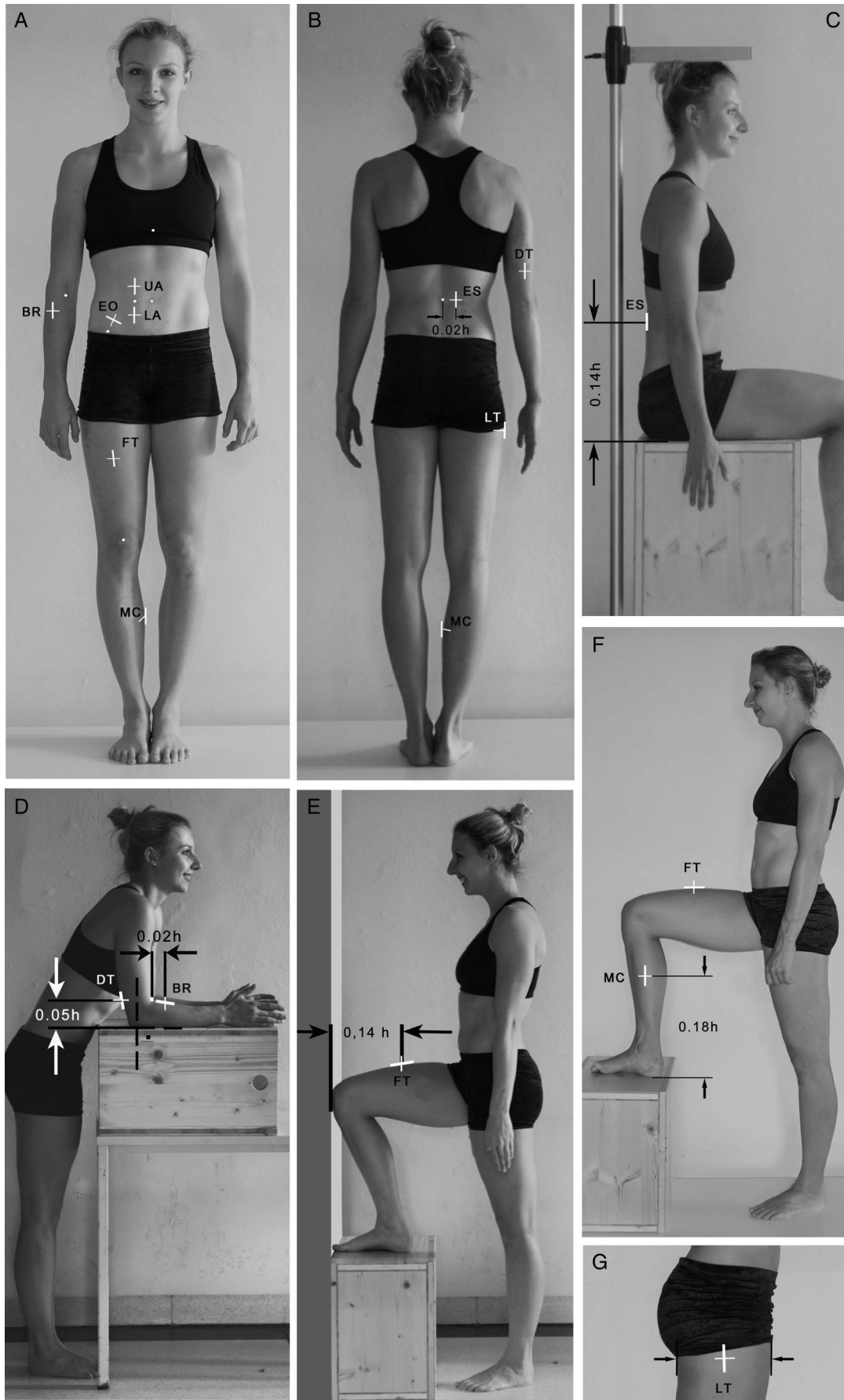
Figure 1 Ultrasound sites. (A and B) Survey of the US sites described in table 1. (C–G) Body positions when marking these sites. (C) shows how to mark the ES site, and also how to measure sitting height (s).

It is important that the participant looks forward at all times when the trunk sites are marked because movements of the head affect marking accuracy. It should also be noted that, while marking is done in a standing or sitting position, all US measurements are made with the participant lying in a supine, prone or rotated position, as described in table 1.

Examples of fat patterning results

A typical US image from the MC site is shown in figure 2. Below the black band corresponding to the gel layer between the probe and skin are the epidermis and dermis, and the dark (almost black) SAT layer (interrupted by a fibrous structure in this case); the fascia of the muscle, and the muscle underneath can be identified easily. The borders of SAT (skin and fascia) are white bands without interruption (no 'black holes' are included in the white bands—this is a necessity for the semiautomatic image segmentation).

A series of US images of a female gymnast, after a phase of reduced training, is shown in figure 3, while figure 4A displays the corresponding SAT thickness values, and figure 4B shows the SAT pattern of the athlete 4 months before when she was in full training. In figure 3, the structures of relevance are easily identifiable: skin, SAT and muscle fascia. At the LA, an intermediate fascia structure is visible (Camper's fascia). In order to determine the precise location of the muscle fascia (the lower border of SAT) in this case, the US probe was applied with varying pressure on the skin (with just a thin layer of gel) before starting the measurement without compression (using a thick layer of gel). The compressibility of SAT is higher than that of muscle tissue and the associated changes in the image due to changing compression enabled the observer to distinguish clearly between them. At the ES site, the thicker skin of the posterior trunk can be seen below the black layer of gel, followed by an almost homogeneous (almost black) SAT layer, and finally the fascia above the muscle appears as a light band. An intermediate fascia is present in this athlete at the FT and MC sites. The seeds from which the SAT contour detection algorithm started are also shown in the images.

Examples of survey plots of the fat patterning in five athletes are shown in figure 4A–F. Figure 4A represents SAT patterning in the female gymnast whose US image series is displayed in

figure 3. D_{INCL} changed by 62% during a phase of reduced training. This large increase in the SAT thickness sum was associated with a weight gain of only 1.4 kg. Figure 4C,D show SAT patterning of two female swimmers; both were preparing for the World Championships in 2015. Between them, SAT thickness sums D_{INCL} differed by 330% (18.0 and 60.6 mm, respectively). Figures 4E (male world champion in swimming) and 4F (international level male gymnast) show extremely low SAT values: the sums of the eight sites D_{INCL} are 9.1 and 6.3 mm, respectively (this equals a mean SAT thickness in these athletes of only 1.1 and 0.8 mm). Body mass index (BMI) does not correlate with sums of SAT thicknesses in the athletes whose SAT thicknesses are shown in figure 4.

Discussion of the site selection and standardisation process

Final selection of the core sites for US SAT patterning studies was a long process. We began with the eight ISAK sites for skinfold measurements because of the existing experiences at these sites.[19] [26–28] A comparison with ISAK skinfolds showed the low validity of skinfold thickness measurements for determining SAT thickness because of the high compressibility of fat.[14] Such accuracy limitations due to the varying compressibility of SAT are to be expected at all other sites that have been used for skinfold measurements as well.[29] Using the individual body height (h) as the distance reference for all sites increases the marking precision substantially and is better than using fixed distance values for all persons independent of their differing body dimensions. Further considerations that influenced the site selection process can be found in online supplementary appendix, part B.

The predictive value of SAT thickness data obtained by US in terms of total body fat remains to be analysed within the framework of validation studies using multicomponent body composition models.[12] [30] The obtainable accuracy (see part A) and precision (see part C) support the expectation that total body fat assessment based on this US technique should result in better adiposity estimates than that based on other field methods, particularly for athletes and other lean individuals in whom internal fat is low.

There is a potential to replace other field methods because of the high accuracy and precision obtainable with US; however, it will take some time until comprehensive reference data become available for comparing and interpreting the results obtained in
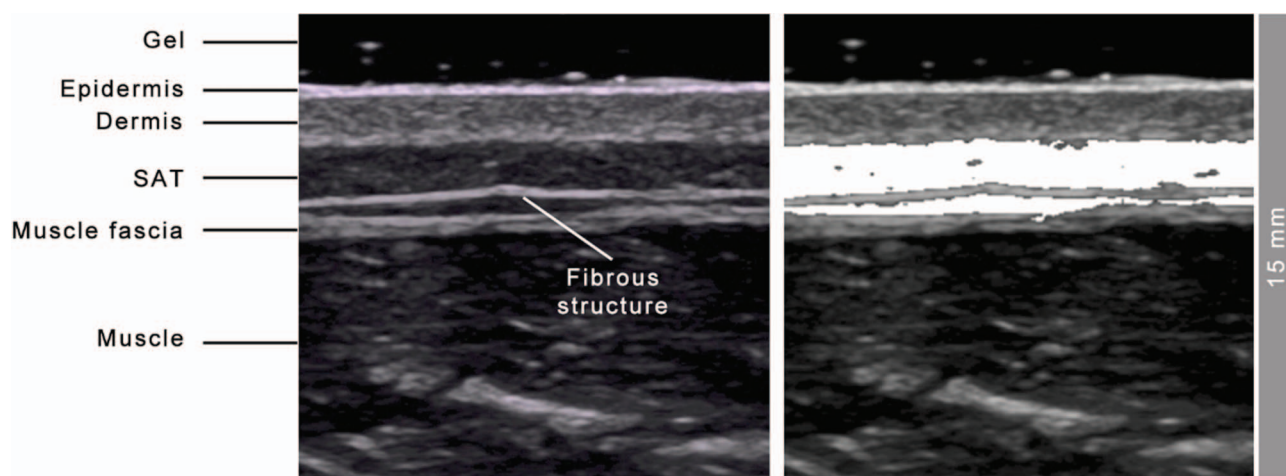

Figure 2 Typical example of an ultrasound image of SAT site: medial calf (MC). Structures of relevance for US image evaluation are marked. In the right-hand image, the detected SAT region is displayed in white. Within the region of interest, the evaluation algorithm measured automatically 280 SAT thickness values (along 280 vertical lines in the image). Means: $D_{INCL}=1.97$ (± 0.14) mm, $D_{EXCL}=1.62$ (± 0.16) mm, and the difference $D_{ES}=0.35$ mm, which represents the mean thickness of the embedded (fibrous) structures. D_{INCL}: thickness with fibrous structures; D_{EXCL}: thickness without fibrous structures. Sound velocity was set to c=1450 m/s. Image depth was 15 mm. SAT, subcutaneous adipose tissue.
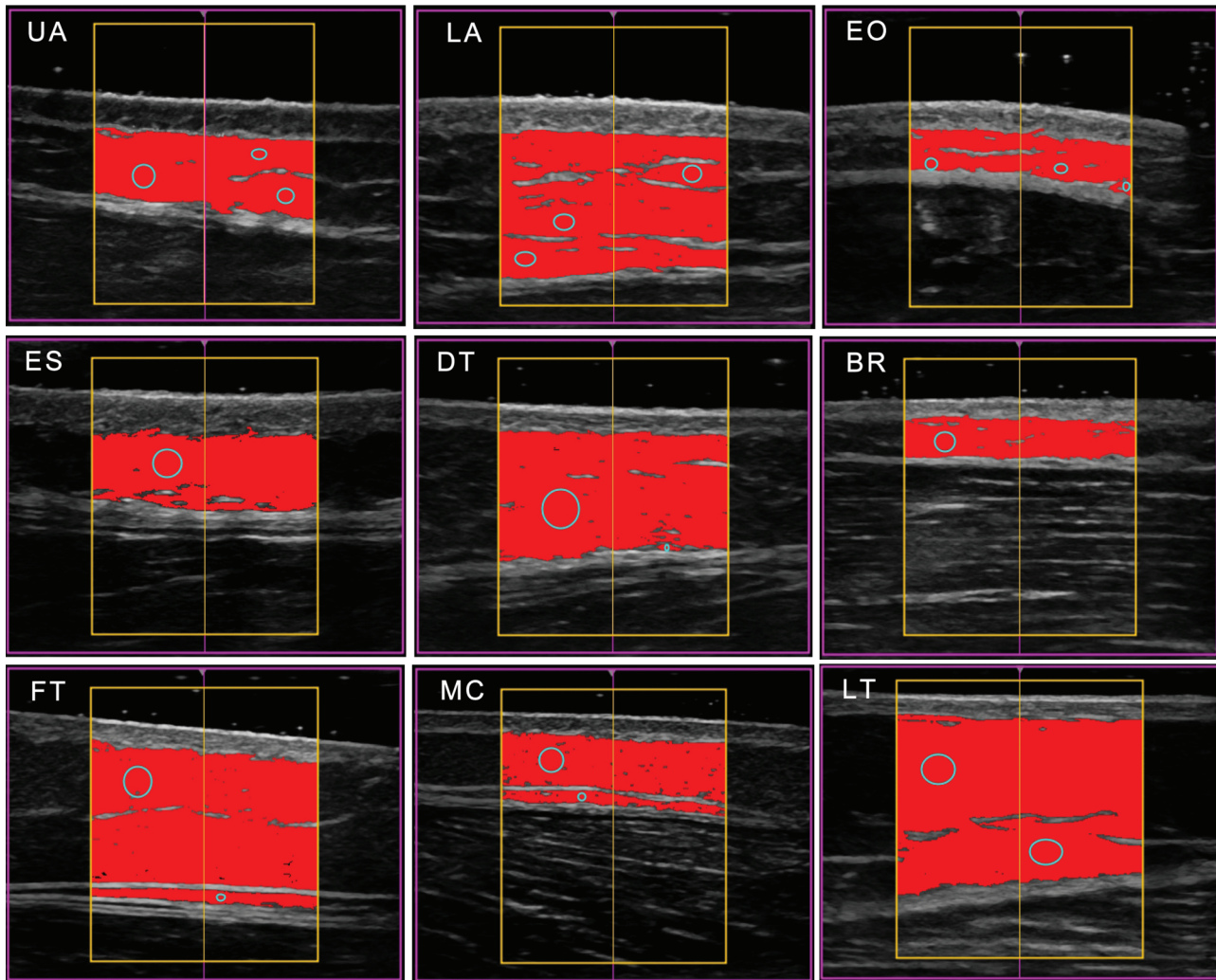
Figure 3 Series of SAT measurements at the sites described in table 1. Typical US images captured for fat patterning analysis. A linear probe (GE, L18) operated at 18 MHz (in harmonic mode) was used. Image depth was 20 mm. Camper's fascia is visible at the lower abdomen (LA) site. Mean SAT thicknesses (in mm) are (compare to figure 4A): UA: 4.26, LA: 8.30, EO: 2.44, ES: 4.29, DT: 7.11, BR: 2.24, FT: 8.99, MC: 4.04, which sum to $D_{INCL}=41.67$ mm in this example. Thickness at LT: 9.85 mm. The mean thicknesses without fibrous structures are: UA: 4.09, LA: 7.30, EO: 2.21, ES: 4.04, DT: 6.84, BR: 2.13, FT: 8.30, and MC: 3.55, and the sum $D_{EXCL}=38.47$ mm; LT: 9.43 mm. UA, upper abdomen; LA, lower abdomen; EO, external oblique; ES, erector spinae; DT, distal triceps; BR, brachioradialis; FT, front thigh; and MC, medial calf; LT, lateral thigh; SAT, subcutaneous adipose tissue.

various groups of athletes. Until then, other field methods may remain in parallel use, although their measurement accuracy does not reach the level desired for medical diagnoses, performance optimisation strategies or 'no-start' decisions.

PART C: INTEROBSERVER RELIABILITY
A comparison of the results obtained by three observers using the standardised US method described in part A and part B is presented in this section. Three observers measured the eight sites each in each of 12 athletes. Each observer evaluated his own 96 images.

METHODS
US sites for measurement of SAT patterning
All sites were marked on the right side of the body. The sites used for this interobserver study were: UA, LA, EO, ES, DT, BR, FT and MC. LT was not used here.

Anthropometry
Anthropometric data included: m, h, sitting height (s)—measured in the fully stretched position, (BMI=m/h²) and the mass

index (MI_1). MI_1 considers individual sitting height: $MI_1=0.53$ m/(hs).[3 4 31] For s/h=0.53, MI_1 equals the BMI.

Statistics, participants and observers
Values are presented as means±SDs and distribution of data is shown in box plots. Further information on statistical methods, participants and observers can be found in online supplementary appendix, part C.

RESULTS
Figure 5 shows the three observers' individual SAT thickness sums D_{INCL} obtained from the eight sites plotted over the mean value of the three observers' sums (in a given athlete). Values are presented in table 2. Online supplementary figure 8 and supplementary table 4 show the results for D_{EXCL}. Sums of SAT thickness measurements with the embedded fibrous structures included are termed D_{INCL}, while D_{EXCL} denotes measurements with the fibrous structures excluded (subtracted). Statistical characteristics for D_{INCL} are: $R^2=0.998$, ICC=0.998, SEE=0.55 mm, and for D_{EXCL}: $R^2=0.997$, ICC=0.996, SEE=0.66 mm. Deviations for D_{INCL} were slightly smaller because there is just one upper border and one lower border to
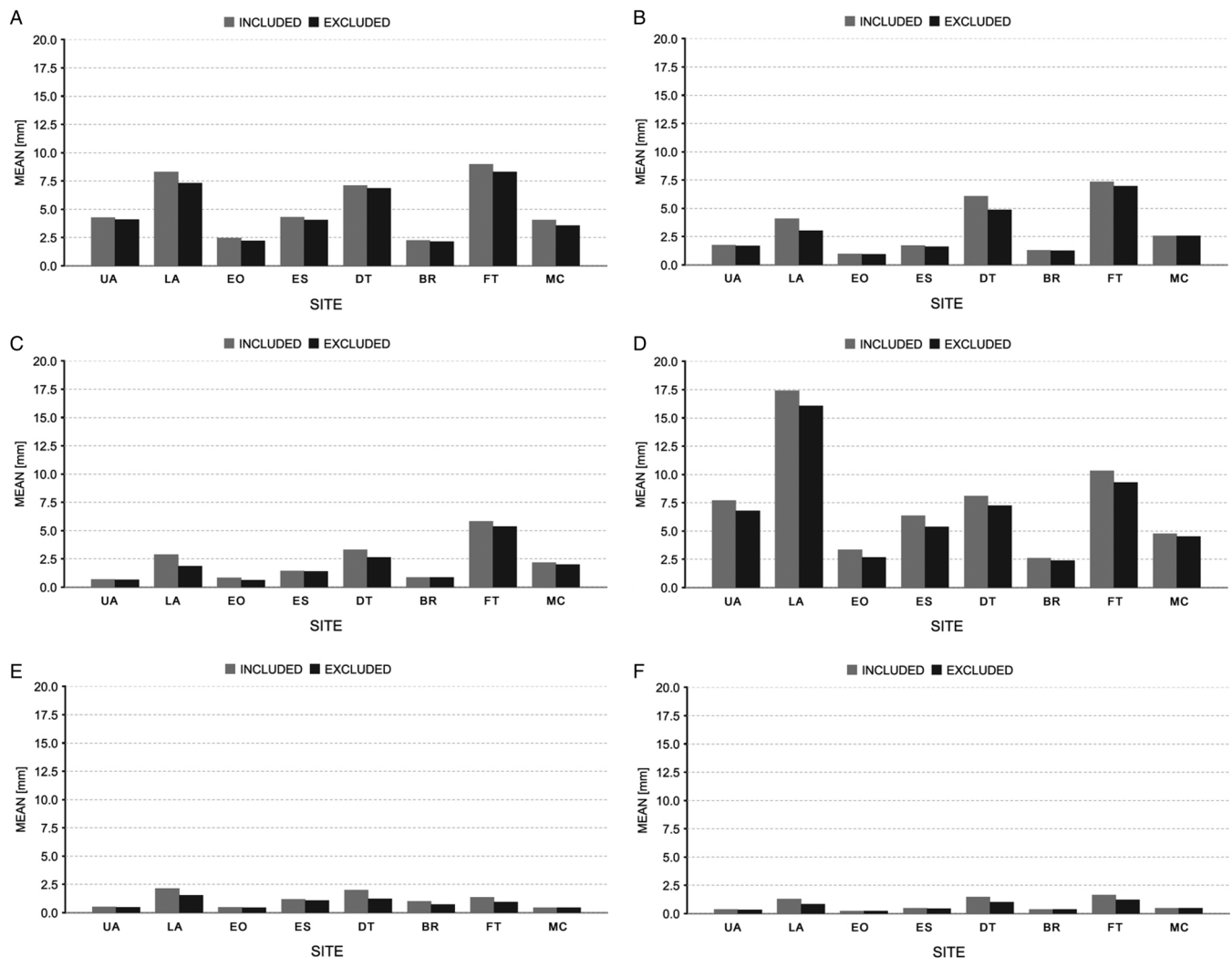
Figure 4 Survey plots of fat patterning in five athletes. The columns show the mean values of the semi-automatic multiple thickness measurements for the eight US sites. The mean thickness value of the SAT thickness in a given ultrasound image (within the region of interest) is termed D_{INCL} (grey) when fibrous structures are included, and it is termed D_{EXCL} (black) when fibrous structures are subtracted. A: Female artistic gymnast in a phase of reduced training (m=59.6 kg, BMI=20.5 kgm^{-2}, D_{INCL}=41.7 mm). B: The same female gymnast 4 months previously when in full training (m=58.2, BMI=20.0 kgm^{-2}, D_{INCL}=25.8 mm). C and D: Female swimmers (m, h, BMI, D_{INCL}: 59.4 kg, 1.685 m; 20.9 kgm^{-2}, 18.0 mm; 67.0 kg, 1.830 m, 20.0 kgm^{-2}, 60.6 mm); both were in preparation for the 2015 world championships. E: World class swimmer (BMI=23.7 kgm^{-2}, D_{INCL}=9.1 mm). F: National level artistic gymnast (BMI=21.4 kgm^{-2}, D_{INCL}=6.3 mm). UA, upper abdomen; LA, lower abdomen; EO, external oblique; ES, erector spinae; DT, distal triceps; BR, brachioradialis; FT, front thigh; and MC, medial calf; LT, lateral thigh.

be determined by the algorithm, whereas for D_{EXCL}, there are several additional borders to be determined to measure the additional thicknesses of embedded structures.

Box plots in figures 6A and 6B represent the absolute values of the individual observer deviations from their means. The three observers measured the sums of eight sites in 12 athletes, resulting in 36 comparisons of SAT thickness sums. Median scores of the absolute deviation values ABS(Δ_{INCL}) and ABS(Δ_{EXCL}) were 0.24 and 0.36 mm, respectively. Maximum deviations of individual observer sums of thicknesses were: ABS($\Delta_{INCL,max}$)=1.50 mm and ABS($\Delta_{EXCL,max}$)=1.58 mm. There are two outliers in each box plot. A comparison of the US images from the three observers showed that an intermediate fascia (Camper's fascia) instead of a muscle fascia had erroneously been used by one observer as the lower border of SAT. The SDs of the observer differences from the mean were: SD(Δ_{INCL})= ±0.54 mm, and SD(Δ_{EXCL})=±0.65 mm, respectively. The 1.96·SD values, representing 95% of measurements, were ±1.1

and ±1.3 mm, respectively (compare with online supplementary figures 9A and 9B).

Box plots in online supplementary figures 9C and 9D represent the distribution of the relative errors Δ_{rel}=100·Δ/D_{MEAN} (in per cent). For $\Delta_{INCL,rel}$, the median is 1.0%, maximum is 3.9%. For $\Delta_{EXCL,rel}$, the median is 1.6%, maximum is 5.3%. The SAT thickness sums for $D_{INCL,MEAN}$ ranged in this group of athletes from 10.2 to 51.2 mm, and for $D_{EXCL,MEAN}$ from 7.3 to 46.7 mm.

The analysis of observer differences at the eight individual sites is described and illustrated in online supplementary figure 10A–D.

DISCUSSION
Interobserver reliability of SAT thickness measurements: results obtained with the new set of sites compared to previous results with ISAK sites
Precision is influenced by the viscoelastic movements of SAT depending on the actual body position during marking and
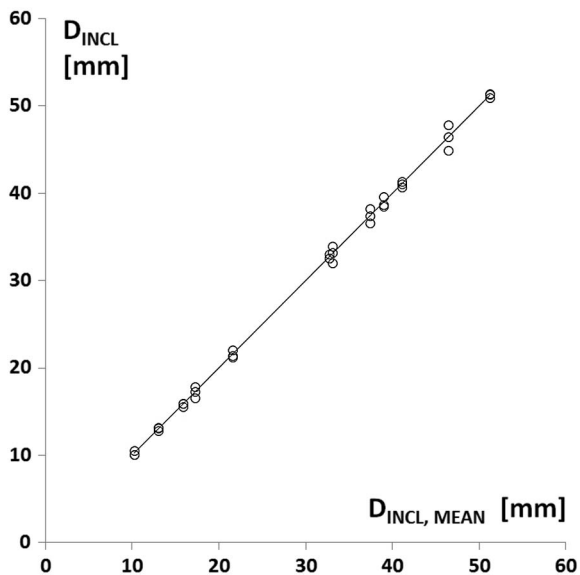
Figure 5 Sums of thicknesses from eight sites measured by the three observers in 12 athletes. The sums D of the individual observers (in a given participant) are displayed over the mean value of the three observers. Sums of SAT thicknesses with the embedded fibrous structures included (D_{INCL}) are shown. $R^2=0.998$ ($p<0.01$), SEE=0.55 mm, ICC=0.998 (lower 95% CI limit: 0.994; upper 95% CI limit: 0.999). SAT, subcutaneous adipose tissue.

during measuring. Standardising the marking and measuring procedure is therefore important to obtain precise results.

Owing to furrowed borders of SAT, precision depends on orientating and positioning the probe at the centre of the site; otherwise, the US image would map another region of SAT (with the high accuracy as discussed in part A) that may have a different thickness, and a different amount of embedded structures. Therefore, it is essential to use measurement sites where the SAT thickness does not change much in the region surrounding the centre of the site. It is of importance that the investigators are trained to find these sites reliably and to apply the method in the standardised way as described in parts A and B of this publication.

Table 2 Measurement results for the three observers

Participant	$D_{INCL, MEAN}$	D_{INCL} OBS1	OBS2	OBS3	Δ_{INCL} OBS1	OBS2	OBS3
1	10.23	10.05	10.07	10.57	−0.18	−0.16	0.34
2	13.02	13.11	12.78	13.16	0.09	−0.24	0.14
3	15.81	15.60	15.89	15.94	−0.21	0.08	0.13
4	17.22	16.54	17.27	17.84	−0.68	0.05	0.62
5	21.57	21.21	22.05	21.44	−0.36	0.48	−0.13
6	32.75	33.05	32.62	32.57	0.30	−0.13	−0.18
7	33.05	32.02	33.94	33.20	−1.03	0.89	0.15
8	37.41	36.59	38.22	37.42	−0.82	0.81	0.01
9	38.96	38.71	39.63	38.54	−0.25	0.67	−0.42
10	41.07	40.73	41.09	41.38	−0.34	0.02	0.31
11	46.43	47.85	44.93	46.50	1.42	−1.50	0.07
12	51.23	51.43	51.33	50.94	0.20	0.10	−0.29

Shown are the sums of SAT thicknesses with embedded structures included (in mm) from eight sites obtained by the three observers in 12 athletes, the means of their measurements and the differences of the individual observer measurements from the means. $D_{INCL,MEAN}$, and $\Delta_{INCL}=D_{INCL}-D_{INCL,MEAN}$ (compare to figure 5 and online supplementary 9A).
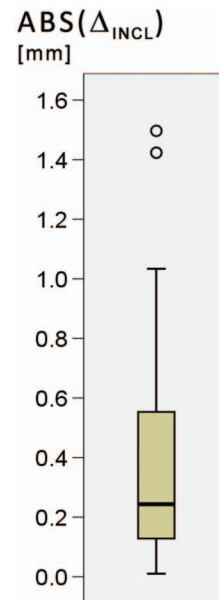SAT, subcutaneous adipose tissue.

Figure 6A Observer differences from the mean. Three observer measurements of the sums from the eight sites in each of the 12 athletes (N=36). The absolute values of the observer differences (their individual sums from eight sites D_{INCL} minus the mean of the three observers $D_{INCL,MEAN}$) are used for this box plot: ABS(Δ_{INCL})=ABS($D_{INCL}-D_{INCL,MEAN}$). Median was 0.24 mm, IQR was 0.46 mm, and maximum deviation from the mean was 1.50 mm.

Comparison of the interobserver studies with ISAK sites and with the new US sites shows that the new sites resulted in much clearer images and higher precision. A detailed comparison of the interobserver reliability obtained with ISAK sites previously[14 15 26] with the results obtained here can be found in online supplementary appendix, part C. Currently, the new sites are being applied within the framework of a multicentre interobserver variability
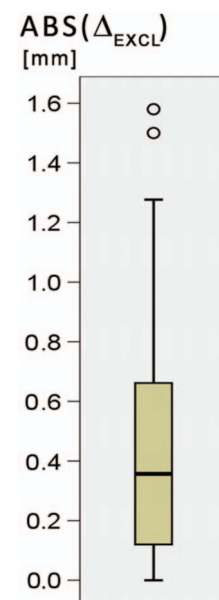

Figure 6B Absolute values of differences (fibrous structures excluded). The absolute values of the individual observer differences (their individual sums from eight sites D_{EXCL} minus the mean of the three observers $D_{EXCL,MEAN}$) were used: ABS(ΔE_{XCL})=ABSD$_{(EXCL-DEXCL,MEAN)}$. Median was 0.36 mm, IQR was 0.57 mm, and maximum deviation from the mean was 1.58 mm.

study under the auspices of the IOC Medical Commission. Comparisons of SAT thickness sums with dual-energy X-ray absorptiometry applied to measure total body fat will also be included in this research.

In the study presented here, the *EO* site was considered because it is situated close to the ISAK site *supraspinale*. However, marking of EO requires palpating and identifying anatomical bony landmarks, whereas all seven other sites do not. In some cases, this caused problems when marking the site precisely, particularly for heavy athletes and in obese persons. A promising candidate for replacing EO is *LT* because at this site interesting information concerning fat patterning in different somatotypes and between men and women can be expected,[27–29] and it is easy to mark LT precisely. The LT site also avoids marking problems that can occur at the EO site in participants with very thick SAT layers. The LT site should therefore replace the EO in future investigations.

SUMMARY AND CONCLUSIONS

All eight new site locations are defined relative to the size of the individual, and a minimum of eight sites are measured to account for inter-individual differences in SAT patterning and for obtaining a sum of SAT thickness which ensures high accuracy and reliability. These new sites optimise the acquisition of clear US images. The orientation of the US probe is approximately parallel with the alignment of the underlying muscle fibres.

To obtain high quality data, observers must participate in a structured training programme that consists of site-marking experience, handling the US system, application of the image segmentation and SAT measurement programme, and guided exercises and interobserver comparisons.

In persons with thick SAT layers, lower frequencies are necessary and they are associated with lower tissue border resolution, but the relative error remains small. Combining the very accurate US method with MRI methods that can be applied to quantify volumes of visceral and abdominal SAT may be the key for developing more enhanced body composition reference methods.[32–35] Furthermore, validation studies against multicomponent models[12 30] are necessary to resolve the question whether SAT thickness measurements with the fibrous structures included or excluded will result in better estimates of total body fat.

The main advantages of this novel US technique over other body composition methods are:

▶ The selected sites represent the relevant body segments: upper and lower abdomen, back, upper arm and forearm, and lateral, upper and lower leg
▶ High measurement accuracy of about 0.2 mm (18 MHz linear probe) can be obtained when the tissue's speed of sound is set correctly
▶ Adipose tissue compression is avoided by using a thick layer of US gel (in addition, the person is asked to stop breathing during image capture)
▶ High precision results when measurers are trained to apply the standardised technique appropriately (95% of SAT thickness sums were within ±1 mm)
▶ Visual control of the semiautomatic measurement algorithm eliminates errors of the automatic contour detection
▶ The automatic measurement of many thickness values in one image, and the possibility to include or exclude embedded structures like fibrous tissues in the thickness values and to quantify their depth
▶ Appropriate for use in the field when employing portable US systems

▶ The technique has minimal subject involvement, does not require ionising radiation and can be applied to children, adolescents and adults
▶ Accommodation of a wide range of adiposity from lean to obese participants
▶ Applying this standardised technique will make results of different working groups directly comparable, and will facilitate the collation of a reference database

At this time, the US technique has the following limitations:

▶ As with skinfolds, this US technique only samples the SAT and does not measure fat stored in the deeper regions
▶ Equipment costs are greater than for skinfolds, but decreasing prices of US systems may accelerate the replacement of other field methods commonly used in sports medicine[36 37]
▶ Since this is a new measurement approach, it will take some time until a comprehensive data pool can be collated. Such a data pool is needed to provide a basis for sports medicine decisions and performance optimisation strategies
▶ The marking, image capture and evaluation of eight sites take about 20 min (which is comparable to skinfolds when eight sites are measured in triplicate).

This US method enables highly sensitive SAT comparisons between individuals and between groups. Various kinds of cross-sectional and longitudinal studies can now be conducted such that small adiposity changes can be detected with the sensitivity that this US technique provides.

What are the findings?

▶ The standardised ultrasound (US) measurement technique enables subcutaneous adipose tissue (SAT) patterning studies with very high accuracy and precision. When sound speed is set correctly, thickness measurement accuracy is approximately 0.2 mm (18 MHz linear US probe).
▶ In athletes, the sum of SAT thicknesses of eight sites varies between a few mm and more than 100 mm. In the interobserver study presented here, it was found that the deviations of three observers' individual measurements from the mean were smaller than ±1 mm in 95% of cases (thickness sums ranged in this group from 10 to 50 mm). Therefore, differences of 2 mm (of the sum from eight sites) could reproducibly be distinguished.
▶ The previously used ISAK sites (International Society for the Advancement of Kinanthropometry), which were defined for skinfold measurements, are not well suited for US imaging of SAT and are therefore replaced by this new set of sites which fulfil the criteria for reproducible and accurate US measurements.
  – UA (upper abdomen),
  – LA (lower abdomen),
  – ES (erector spinae),
  – DT (distal triceps),
  – BR (brachioradialis),
  – LT (lateral thigh),
  – FT (front thigh),
  – MC (medial calf).
▶ All new sites overlie muscle with a clearly visible fascia, away from other complex structures, thus easing the acquisition of US images. SAT layers show little variation in thickness in the vicinity of these selected sites; this is an important criterion because the major part of measurement deviations is due to unavoidable position changes of the US probe when measurements are repeated.
▶ Fibrous structures embedded in SAT can also be quantified.

Original article

How might it impact on clinical practice in the future?

- This new US method is capable of measuring SAT layers without compression and with high accuracy and precision. Therefore, it enables longitudinal studies of fat patterning changes and athlete comparisons with a sensitivity not reached by any other technique.
- This US measurement approach will complement other laboratory methods, and it is also applicable for use in the field.
- There is potential for US to replace other field methods because of its high accuracy and precision; however, it will take some time until comprehensive reference data of various groups of athletes will be available.
- This US technique provides the highest technically obtainable accuracy for SAT thickness measurement, which is limited only by biological factors. The new site definitions improve the application of US and result in good reliability.
- The semiautomatic image evaluation also allows the quantitative determination of the amount of fibrous structures embedded in SAT, which varies largely from one site to another and between individuals.
- Owing to the high accuracy of image evaluation, this US method can also be applied to optimise the image segmentation algorithms of other imaging techniques like MRI or CT.
- This emerging measurement technique has the potential to spread rapidly because prices of high-quality US imaging systems have decreased markedly in recent years.
- The eight selected sites can be used as a standard set of sites for pooling data on SAT patterning in athletes (and in untrained persons) which will be valuable for comparisons of SAT layers among individuals and between groups.
- Specific training of US imaging and evaluation of SAT is necessary to obtain high reproducibility and accuracy of measurements. Two days of training are sufficient for measurers who have had some prior US imaging experience.

ABBREVIATIONS:

OBS	Observer
SAT	Subcutaneous adipose tissue
US	Ultrasound

Parameters and variables:

m	Body mass, in kg
h	Body height (stature) in m
s	Sitting height, in m
BMI	Body mass index: BMI=m/h^2, in kgm^{-2}
MI_1	Mass index: $MI_1=0.53 \cdot m/(hs)$, in kgm^{-2}
d	SAT thickness measured by an individual observer at a given site, in mm (this is the average of the distances measured within the region of interest)
D	Sum of SAT-thicknesses measured by an individual observer at all eight sites in a given participant, in mm
δ	measurement deviation of an individual observer from the mean of the three observers at a given site in a given athlete, in mm
δ_{rel}	$\delta_{rel}= 100 \cdot \delta/d_{MEAN}$, in [%]
Δ	Deviation of the sum of eight sites measured by an individual observer from the mean of the sums of the three observers in a given athlete, in mm
Δ_{rel}	$\Delta_{rel}= 100 \cdot \Delta/D_{MEAN}$, in [%]
EXCL	Excluded; indicates that the fibrous structures embedded in the SAT are not included in the thickness value.
INCL	Included; indicates that the fibrous structures are included
c	speed of sound

Statistics:

N	Number of values
ABS	Absolute value of a number
MEAN	Mean value
SD	Standard deviation
SEE	Standard error of estimate
ICC	Intraclass correlation coefficient
IQR	Interquartile range
R^2	Coefficient of determination
ρ	Spearman's rank correlation coefficient (Spearman's rho)

Ultrasound sites:

UA	Upper abdomen
LA	Lower abdomen
ES	Erector spinae
DT	Distal triceps
BR	Brachioradialis
FT	Front thigh
LT	Lateral thigh
MC	Medial calf
EO	External oblique

REFERENCES

1 Nattiv A, Loucks AB, Manore MM, et al, American College of Sports Medicine. American College of Sports Medicine position stand. The female athlete triad. Med Sci Sports Exerc 2007;39:1867–82.

2 Byrne S, McLean N. Eating disorders in athletes: a review of the literature. J Sci Med Sport 2001;4:145–59.

3 Müller W. Determinants of ski jump performance and implications for health, safety and fairness. Sports Med 2009;39:85–106.

4 Müller W. Towards research based approaches for solving body composition problems in sports: ski jumping as a heuristic example. Br J Sports Med 2009;43:1013–19.

5 Sundgot-Borgen J, Meyer NL, Lohman TG, et al. How to minimise the health risks to athletes who compete in weight-sensitive sports review and position statement on behalf of the Ad Hoc Research Working Group on Body Composition, Health and Performance, under the auspices of the IOC Medical Commission. Br J Sports Med 2013;47:1012–22.

6 Becker AE, Grinspoon SK, Klibanski A, et al. Current concepts: eating disorders. N Engl J Med 1999;340:1092–8.

7 Sullivan PF. Mortality in anorexia nervosa. Am J Psychiatry 1995;152:1073–4.

8   Fogelholm M. Effects of bodyweight reduction on sports performance. *Sports Med* 1994;18:249–67.

9   Tofler IR, Stryer BK, Micheli LJ, *et al*. Physical and emotional problems of elite female gymnasts. *N Engl J Med* 1996;335:281–3.

10 Alderman BL, Landers DM, Carlson J, *et al*. Factors related to rapid weight loss practices among international-style wrestlers. *Med Sci Sports Exerc* 2004;36:249–52.

11 Mountjoy M, Sundgot-Borgen J, Burke L, *et al*. The IOC consensus statement: beyond the Female Athlete Triad—Relative Energy Deficiency in Sport (RED-S). *Br J Sports Med* 2014;48:491–7.

12 Ackland TR, Lohman TG, Sundgot-Borgen J, *et al*. Current status of body composition assessment in sport: review and position statement on behalf of the Ad Hoc Research Working Group on Body Composition Health and Performance, under the auspices of the I.O.C. Medical Commission. *Sports Med* 2012;42:227–49.

13 Müller W, Maughan RJ. The need for a novel approach to measure body composition: is ultrasound an answer? *Br J Sports Med* 2013;47:1001–2.

14 Müller W, Horn M, Fürhapter-Rieger A, *et al*. Body composition in sport: a comparison of a novel ultrasound imaging technique to measure subcutaneous fat tissue compared with skinfold measurement. *Br J Sports Med* 2013;47:1028–35.

15 Müller W, Horn M, Fürhapter-Rieger A, *et al*. Body composition in sport: inter-observer reliability of a novel ultrasound measure of subcutaneous fat. *Br J Sports Med* 2013;47:1036–43.

16 El-Brawany MA, Nassiri DK, Terhaar G, *et al*. Measurement of thermal and ultrasonic properties of some biological tissues. *J Med Eng Technol* 2009;33:249–56.

17 Herman IP. *Physics of the human body*. Berlin: Springer-Verlag, 2007:559.

18 Bullen BA, Quaade F, Olsen F, *et al*. Ultrasonic reflections used for measuring subcutaneous fat in humans. *Hum Biol* 1965;37:375–84.

19 Booth RAD, Goddard BA, Paton A. Measurement of fat thickness in man: a comparison of ultrasound, Harpenden calipers and electrical conductivity. *Br J Nutr* 1966;20:719–25.

20 Bellisari A. Sonographic measurement of adipose tissue. *J Diagn Med Sonogr* 1993;9:11–8.

21 Ramirez ME. Measurement of subcutaneous adipose tissue using ultrasound images. *Am J Clin Anthropol* 1992;89:347–57.

22 Bellisari A, Roche AF, Siervogel RM. Reliability of B-mode ultrasonic measurements of subcutaneous adipose tissue and intra-abdominal depth: comparisons with skinfold thickness. *Int J Obes Relat Metab Disord* 1993;17:475–80.

23 Bellisari A, Roche AF. Anthropometry and ultrasound. In: Heymsfield SB, Lohman TG, Wang ZM, *et al.*, eds. *Human body composition*. 2nd edn. Champaign, IL: Human Kinetics, 2005:109–27.

24 Koda M, Senda M, Kamba M, *et al*. Sonographic subcutaneous and visceral fat indices represent the distribution of body fat volume. *Abdom Imaging* 2009;32:387–92.

25 Himes JH, Roche AF, Siervogel RM. Compressibility of skinfolds and the measurement of subcutaneous fatness. *Am J Clin Nutr* 1979;32:1734–40.

26 Stewart A, Marfell-Jones M, Olds T, *et al*. *International standards for anthropometric assessment*. Lower Hutt, New Zealand: International Society for the Advancement of Kinanthropometry, 2011.

27 Stewart AD, Sutton L. *Body composition in sport, exercise and health*. Abingdon, UK: Routledge, 2012.

28 Stewart AD. Anthropometric fat patterning in male and female subjects. In: Reilly T, Marfell-Jones M, eds. *Kinanthropometry VIII: proceedings of the 8th international society for the advancement of kinanthropometry conference*. London: Routledge, 2003:195.

29 Raschka C. Sportanthropologie. 1st edition, Kölu: Sportverlag Srauß. 2006:104.

30 Wang Z, Shen W, Withers RT, *et al*. Multicomponent molecular-level models of body composition analysis. In: Heymsfield SB, Lohman TG, Wang ZM, *et al*, eds. *Human body composition*. 2nd edn. Champaign, IL: Human Kinetics, 2005: 163–76.

31 Müller W, Gröschl W, Müller R, *et al*. Underweight in ski jumping: the solution of the problem. *Int J Sports Med* 2006;27:926–34.

32 Bosy-Westphal A, Booke CA, Blöcker T, *et al*. Measurement site for waist circumference affects its accuracy as an index of visceral and abdominal subcutaneous fat in a Caucasian population. *J Nutr* 2010;140:954–61.

33 Thomas DM, Bredlau C, Bosy-Westphal A, *et al*. Relationships between body roundness with body fat and visceral adipose tissue emerging from a new geometrical model. *Obesity* 2013;21:2264–71.

34 Shen W, Chen J, Gantz M, *et al*. A single MRI slice does not accurately predict visceral and subcutaneous adipose tissue changes during weight loss. *Obesity* 2012;20:2458–63.

35 Shen W, Punyanitya M, Silva AM, *et al*. Sexual dimorphism of adipose tissue distribution across the lifespan: a cross-sectional whole-body magnetic resonance imaging study. *Nutr Metab* 2009;6:17.

36 Meyer NL, Ackland TR, Lohman TG, *et al*. Body composition for Health and Performance: A Survey of the Ad Hoc Research Working Group on Body Composition, Health and Performance, under the auspices of the I.O.C. Medical Commission. *Br J Sports Med* 2013;47:1044–53.

37 Santos D, Dawson JA, Matias CN, *et al*. Reference values for body composition and anthropometric measurements in athletes. *PLoS ONE* 2014;9:e97846.

BJSM

Subcutaneous fat patterning in athletes: selection of appropriate sites and standardisation of a novel ultrasound measurement technique: ad hoc working group on body composition, health and performance, under the auspices of the IOC Medical Commission

Wolfram Müller, Timothy G Lohman, Arthur D Stewart, Ronald J Maughan, Nanna L Meyer, Luis B Sardinha, Nuwanee Kirihennedige, Alba Reguant-Closa, Vanessa Risoul-Salas, Jorunn Sundgot-Borgen, Helmut Ahammer, Friedrich Anderhuber, Alfred Fürhapter-Rieger, Philipp Kainz, Wilfried Materna, Ulrike Pilsl, Wolfram Pirstinger and Timothy R Ackland

---

Updated information and services can be found at:
http://bjsm.bmj.com/content/50/1/45

These include:

Supplementary Material

Supplementary material can be found at:
http://bjsm.bmj.com/content/suppl/2015/12/22/50.1.45.DC1.html

References

This article cites 30 articles, 9 of which you can access for free at:
http://bjsm.bmj.com/content/50/1/45#BIBL

Open Access

Email alerting service

Receive free email alerts when new articles cite this article. Sign up in the box at the top right corner of the online article.

Topic Collections

Articles on similar topics can be found in the following collections

Open access (211)

To request permissions go to:
http://group.bmj.com/group/rights-licensing/permissions

To order reprints go to:
http://journals.bmj.com/cgi/reprintform

To subscribe to BMJ go to:
http://group.bmj.com/subscribe/

Notes